Effects of cytochalasin D and latrunculin B on mechanical properties of cells

Tetsuro Wakatsuki, Bill Schwab, Nathan C. Thompson and Elliot L. Elson*

Department of Biochemistry and Molecular Biophysics, Washington University School of Medicine, St. Louis, MO 63110, USA
*Author for correspondence (e-mail: elson@biochem.wustl.edu)

Accepted 19 December 2000
Journal of Cell Science 114, 1025-1036 © The Company of Biologists Ltd

SUMMARY

Actin microfilaments transmit traction and contraction forces generated within a cell to the extracellular matrix during embryonic development, wound healing and cell motility, and to maintain tissue structure and tone. Therefore, the state of the actin cytoskeleton strongly influences the mechanical properties of cells and tissues. Cytochalasin D and Latrunculin are commonly used reagents that, by different mechanisms, alter the state of actin polymerization or the organization of actin filaments. We have investigated the effect of a wide range of Cytochalasin D and Latrunculin B concentrations (from 40 pM to 10 μM) on the mechanical properties of the cells within fibroblast populated collagen matrices. Contractile force and dynamic stiffness were measured by uniaxial stress-strain testing. The range of effective concentrations of Cytochalasin D (200 pM-2 μM) was broader than that of Latrunculin B (20 nM-200 nM). Activating the cells by serum did not change the effective range of Cytochalasin D concentrations but shifted that of Latrunculin B upward by tenfold. Simple mathematical binding models based on the presumed mechanisms of action of Cytochalasin D and Latrunculin B simulated the concentration-dependent mechanical changes reasonably well. This study shows a strong dependence of the mechanical properties of cells and tissues on the organization and degree of polymerization of actin filaments.

Key words: Viscoelasticity, Collagen gel, Cell indentation, Cytochalasin D

INTRODUCTION

Comparative rheological studies of isolated actin filaments, microtubules and intermediate filaments indicate that actin filaments should have a preponderant role in controlling cell shape and mechanical properties at physiological strain levels (Janmey et al., 1991). Cellular stiffness and the development of contractile force require actin filaments (Elson, 1988). Therefore measurements of stiffness and force can directly indicate the physical state of the actin cytoskeleton. The physical properties of individual actin filaments and their organization into networks and bundles determine the mechanical characteristics of this filament system. The mechanical properties of both single actin filaments (Kojima et al., 1994; Tsuda et al., 1996) and bulk polymer networks (Janmey et al., 1994; Ziemann et al., 1994) have been studied in vitro. Moreover, actin polymerization and its regulation in living cells have been studied extensively. Many biochemical parameters involved in these processes have been measured in vitro (Carlier, 1998; Mullins et al., 1998; Pollard and Cooper, 1986). The dependence of the mechanical properties of living cells on the organization of their actin cytoskeletons has, however, been systematically examined using only atomic force microscopy (AFM) (Rotsch and Radmacher, 2000).

Cytochalasin D (CD) provides a convenient and powerful method for perturbing the actin cytoskeleton. CD has been used to test the involvement of actin polymerization in cellular activities and properties such as cell motility (Pelham and Wang, 1999), contraction (Kolodney and Wysolmerski, 1992) and cell stiffness (Elson et al., 1984; Wang et al., 1993), and to examine the functions of specific proteins, e.g. the actin capping protein (Schafer et al., 1998). The dissociation constant of CD on isolated actin filaments (2 nM) is nearly 1000 times less than concentration typically used to disrupt actin filaments in cells (1-2 μM) (Cooper, 1987).

The mechanical properties of nonmuscle cells can be measured with high precision and reproducibility using cell-populated reconstituted tissue models, Fibroblast Populated Matrices (FPMs; Wakatsuki et al., 2000). This approach has the advantage over single-cell methods (Elson et al., 1984; Putman et al., 1994; Thoumine and Ott, 1997; Wang et al., 1993) that the cells are in a relatively natural three-dimensional extracellular matrix and that each measurement samples the properties of a population of cells, thereby averaging over substantial cell-to-cell variations. As described previously (Wakatsuki et al., 2000), we have measured the effects of a range of CD concentrations on the cell-dependent mechanical properties of FPMs. The sensitivity of our measurement allowed us to determine quantitatively the small changes in FPM mechanical properties caused by CD concentrations as low as 2 nM. The half-maximal change in mechanical properties occurred at a CD concentration of ~0.25 μM, 100-fold higher than the dissociation constant of CD measured on isolated actin filaments. This discrepancy could be explained by competition between CD and capping protein localized at membrane adhesion sites to bind to the barbed ends of actin

filaments. As reviewed by Vaheri et al. (Vaheri et al., 1997), the subfamily of ERM proteins (ezrin/radixin/moesin) in the band 4.1 superfamily (Sato et al., 1992) could link the barbed ends actin filaments to the plasma membrane. Ezrin binds indirectly to the barbed ends of actin filaments via the capping protein, βCAP73 (Shuster and Herman, 1995; Shuster et al., 1996). Tensin localized at focal contacts could also link the membrane to the actin cytoskeleton. Its multiple actin binding sites include one that caps barbed ends of actin filaments (Kd=20 nM) (Lo et al., 1994b). To illustrate the above hypothesis we have constructed a steady-state model that correlates the displacement of the barbed-ends of the actin filaments from their cellular binding sites by CD, with changes in cellular mechanical properties. The model rationalizes the high concentration of CD needed to disorganize completely the actin cytoskeleton in cells. The competition model also simply explains the wide range over which CD causes mechanical changes in FPMs in terms of populations of capping proteins with different affinities for actin filaments. The model presented here is still primitive; yet it simulates the data with reasonable constants chosen from the literature.

The marine toxins latrunculin A and B (LA-A and LA-B) form 1:1 complexes with actin monomers and thereby inhibit actin polymerization (Coue et al., 1987; Spector et al., 1989). In measurements on FPMs, we have observed that, in contrast to CD, the concentrations of LA-B effective for disrupting the actin cytoskeleton in living cells are comparable with the binding constant measured on isolated actin monomers (0.2 μM). Moreover, we have observed that activation of fibroblasts in FPMs by calf serum does not change the dependence of mechanical properties on CD concentration but displaces upwards the effective concentrations of LA-B. These results shed light on the mechanisms of action of CD and LA-B in cells and provide an example of how measurements of the mechanical properties of reconstituted tissue models can be used to assess the state of the cytoskeletons of the cells within the tissues.

MATERIALS AND METHODS

Cell and tissue culture

The methods for producing FPMs and measuring their mechanical properties are described in detail elsewhere (Wakatsuki et al., 2000). Briefly, chicken embryo fibroblasts (CEFs) were maintained in Dulbecco's modified Eagle's medium (DMEM) supplemented with 10% fetal calf serum (FCS), penicillin (50 units/ml) and streptomycin (50 mg/ml). The trypsinized cells were mixed with monomeric collagen and an appropriate growth medium to yield a suspension containing 10^6 cells/ml. 1 ml of this solution was poured into each of several casting wells made from Teflon and these were incubated at 37°C with 5% CO_2 for 2 days. The collagen is in an annular space between the inner wall of the cylindrical casting well and a central mandrel. The collagen polymerizes at 37°C to form a gel. Over the course of 2 days in culture the cells compress the collagen around the mandrel to a thickness of 200-300 μm, ~10% of its original volume. This thin ring of tissue is easily removed from the mandrel at the end of the incubation period. For the last 12 to 16 hours prior to measurements, the FPMs were incubated in the absence of FCS.

Mechanical measurements of the FPMs

After the FPM ring was gently removed from the mandrel, it was connected to an isometric force transducer (model 52-9545, Harvard Apparatus, South Natick, MA) and a stepper motor (P/N 1-19-3400 24V DC 1.8 deg step size, Haward Industry, MO) controlled by a microstepping driver (IM483 Intelligent Motion Systems, Inc., Marlborough, CT). The FPM was submerged in 50 ml Hepes-buffered DMEM in a thermo-regulated organ bath (Harvard Apparatus, South Natick, MA) maintained at 37°C and at pH 7.4. With the FPM at its original contour length, L_0, i.e. initial strain=0, dynamic stiffness was measured by subjecting the FPM to a small sinusoidal strain. Even though reconstituted tissues are mechanically nonlinear, the application of a sufficiently small sinusoidal strain (dL/L_0) yields a sinusoidal force response. Hence, for the very small strains used in these experiments, the tissue equivalents appear linear. The dynamic stiffness was measured as the amplitude of the force response/corresponding strain (20 μm amplitude; less than 0.5% strain, 0.5 Hz frequency). Isometric force and dynamic stiffness were measured once the force reached a steady level after the treatments by CD or LA, which is typically ~30 minutes.

Indentation stiffness measurements of single cells

A vertical glass stylus with a tip about 2 μm in diameter was connected to a linear piezoelectric motor by a glass beam of known bending constant. The vertical position of the stylus tip was monitored optically by measuring the light reflected from a flag attached to the tip. The force exerted on the tip by the resistance of the cell to the indentation was calculated by measuring the bending of the beam (Zahalak et al., 1990).

Phase angle and viscosity

A part of the energy required to strain the FPM is dissipated by the viscosity of the tissue model. The FPMs were subjected to uniaxial cyclic stretch with amplitude and frequency of 20 μm and 0.5 Hz, respectively. The force response to the sinusoidal strain was also sinusoidal but delayed by phase angle δ. The phase angle provides an indicator of viscosity of the tissue models. The phase angles were calculated using the Fast Fourier Transform (FFT) program provided by Origin software (Microcal Software, Northampton, MA).

Fluorescence microscopy

A monolayer containing ~100,000 CEF was cultured overnight on 35 mm^2 tissue-culture dishes with DMEM with 10% FCS. CD and LA-B were added to the monolayers in DMSO. The amount of DMSO in no case exceeded 0.1% of the total volume of the medium. After a minimum of 30 minutes exposure to CD or LA-B, the dishes were washed quickly with PBS and fixed with 5% paraformaldehyde solution in PBS for 10 minutes at room temperature. The actin filaments were stained with rhodamine phalloidin (Sigma, St. Louis, MO). The fluorescent images of actin filaments were taken using scanning confocal microscopy (BioRad, Hercules, CA).

RESULTS

F-actin distribution in the CEF after treatment with different doses of CD or LA-B

CEF monolayers were treated with concentrations of CD ranging from 40 pM to 2 μM for at least 30 minutes and fixed with formaldehyde. Fluorescence micrographs of the actin cytoskeletons, stained with rhodamine-phalloidin, were obtained by scanning confocal microscopy (Fig. 1). Visible changes in the actin cytoskeleton were detectable when the CD concentration reached 20 nM (Fig. 1E). At this concentration, small actin aggregates co-existed with actin microfilament bundles and diffuse cortical F-actin. At a CD concentration of 2 μM almost all the long actin filament bundles had been disrupted and replaced by large focal aggregates of F-actin (Fig. 1H). Typically, CD is used at 2 μM to disrupt the actin

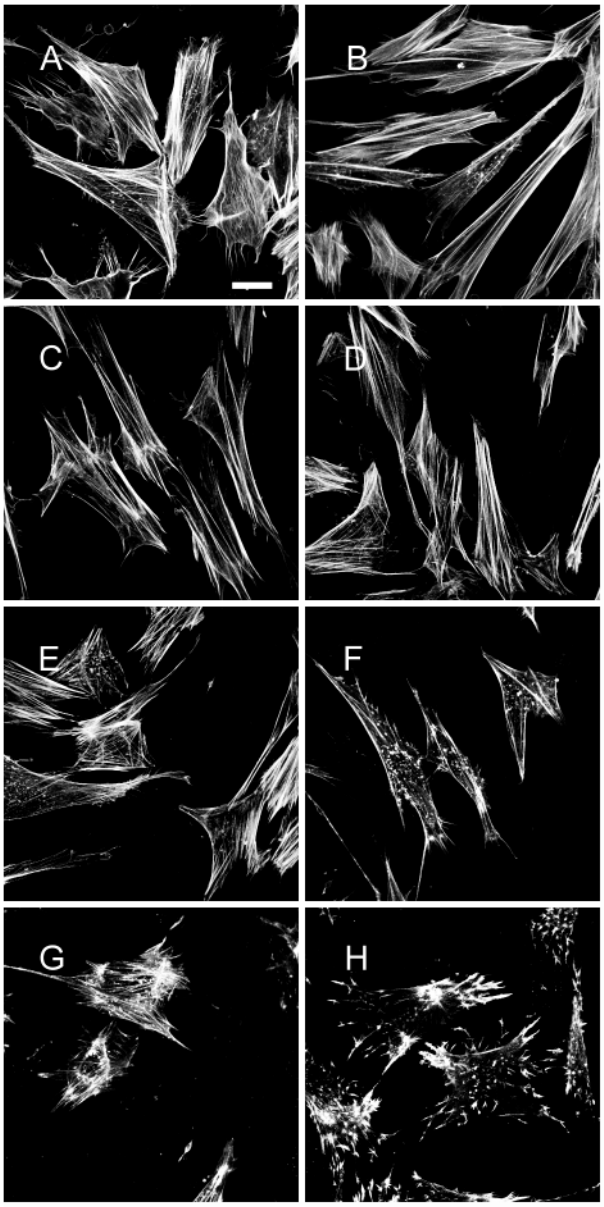

Fig. 1. Changes in the organization of the actin cytoskeleton at various concentrations of CD. The actin cytoskeletons of CEF cultured in monolayers on coverslips in the presence of 10% FCS were stained with rhodamine-phalloidin. The cells were incubated with 0.1% DMSO (control, A), 200 pM (B), 900 pM (C), 4 nM (D), 20 nM (E), 90 nM (F), 400 nM (G) and 2 μM (H) of CD for 30 minutes. Visible changes in the actin cytoskeleton did not appear until the CD concentration reached 20 nM (D). At this concentration, small actin aggregates co-existed with actin microfilament bundles and diffuse cortical F-actin. At a CD concentration of 2 μM (G), almost all the long actin filaments were disrupted and replaced by large focal aggregates of F-actin. Scale bar: 50 μm.

cytoskeleton (Kolodney and Wysolmerski, 1992; Pelham and Wang, 1999). Fig. 1 clearly demonstrates that this concentration of CD causes a major disruption of the actin cytoskeleton.

Actin cytoskeletons of CEF monolayers treated with concentrations of LA-B ranging from 10 nM to 10 μM were visualized similarly as the samples treated with CD (Fig. 2). No visible changes were observed until the concentration of LA-B

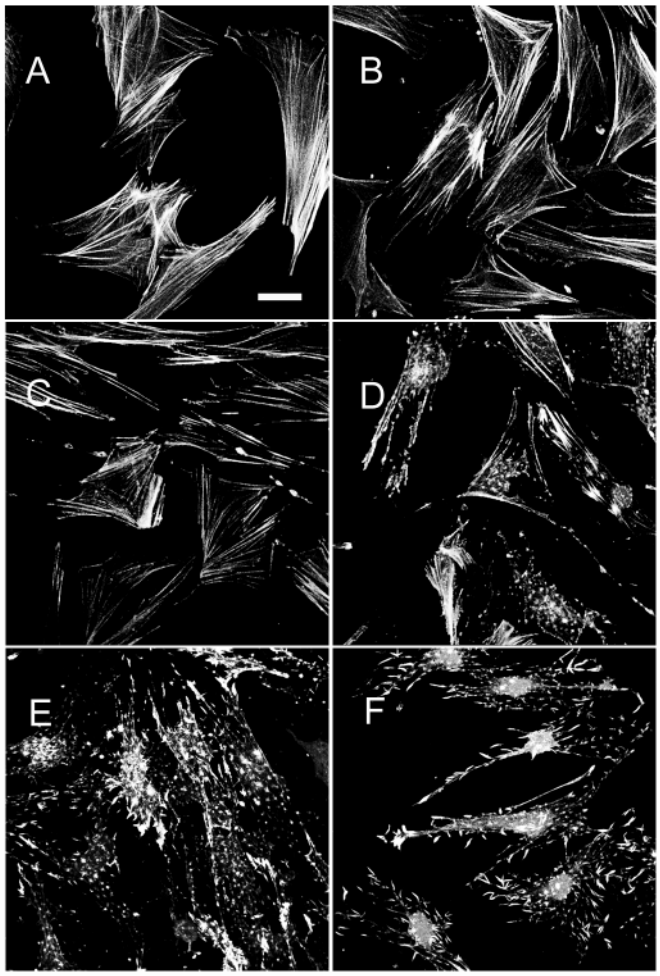

Fig. 2. Changes in the organization of the actin cytoskeleton at various concentrations of LA-B. CEF cultured as for Fig. 1 (with FCS) were incubated with 10 nM (A), 40 nM (B), 160 nM (C), 630 nM (D), 2 μM (E) and 10 μM (F) of LA-B for 30 minutes. Then, they were fixed and stained with rhodamine-phalloidin and imaged by scanning confocal microscopy. Significant visible changes in the actin cytoskeleton did not appear until the LA-B concentration reached 630 nM (D). At this concentration many small actin aggregates coexisted with cortical F-actin. At a LA-B concentration of 2 μM (E) almost all the long actin filaments were disrupted and replaced by large focal aggregates of F-actin. The concentration range over which actin filaments were disrupted was much smaller for LA-B than for CD. Scale bar: 50 μm.

reached 160 nM (Fig. 2D). At 630 nM (Fig. 2E) actin filament bundles were mostly replaced by actin aggregates. A transition from long F-actin filament bundles to the aggregated state seemed to occur over a narrow range of LA-B concentration.

CD and LA-B dose-dependent mechanical properties

The isometric tension and the dynamic stiffness of 2-day-old FPMs, which have been serum starved for 16 hours prior to the experiment, were measured over a range of CD concentrations. The measurements were carried out serially on each FPM, beginning with the lowest concentration of CD. For each FPM, CD was added and force and stiffness were measured and then the process was repeated with the next higher CD

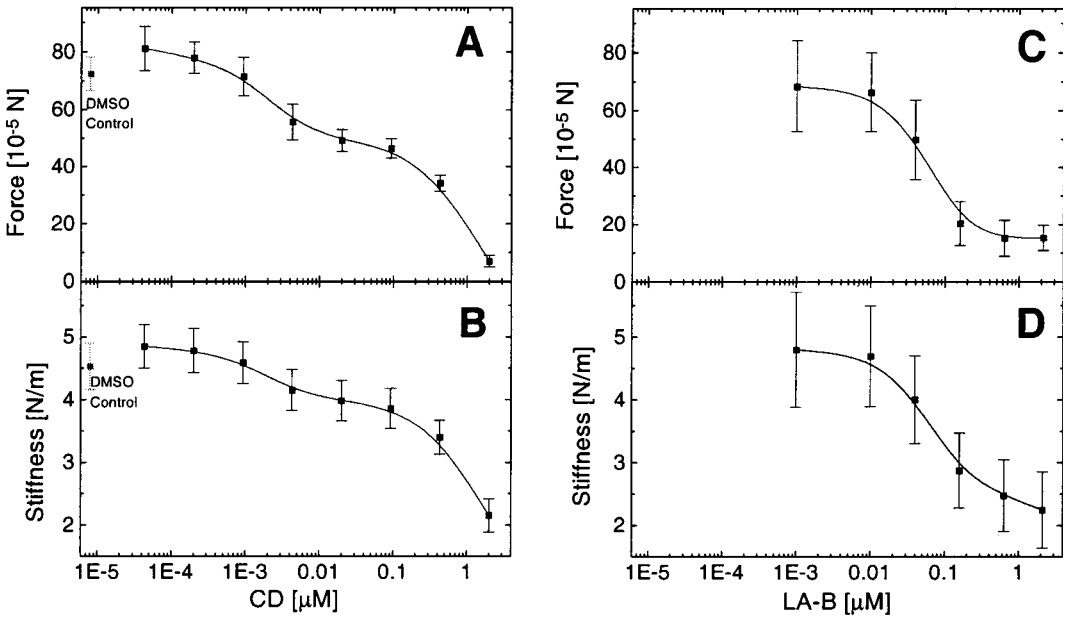

Fig. 3. Dependence of force and dynamic stiffness on CD and LA-B concentrations. The force and dynamic stiffness were significantly diminished at a CD concentration of 2 nM and continued to fall as the CD concentration was increased (A,B). In contrast, for LA-B the force and dynamic stiffness began to diminish only when the concentration reached 40 nM, and reached their minimum values at a concentration of ~600 nM (C, D).

concentration (Fig. 3A,B). The total amount of DMSO added was less than 0.1% of the total volume of the DMEM. This quantity of DMSO had no significant effect on the force and stiffness of FPMs. The data shown were averaged over quadruplicated samples, and the same experiment was repeated at least twice. The force and dynamic stiffness were significantly decreased at a CD concentration as low as 2 nM. At this concentration, no effect was observed by confocal microscopy on the actin cytoskeletons in monolayer cultures (Fig. 1B). Both force and dynamic stiffness continued to decrease as the CD concentration increased up to 2 μM. At this concentration, the force was reduced almost to zero and the stiffness had nearly reached its minimum value. For CD concentrations higher than 2 μM, the stiffness did not significantly diminish further (data not shown). The concentration of CD needed to reduce the force and dynamic stiffness by 50% was approximately 0.25 μM (Table 1).

Measurements of the effects of LA-B on the mechanics of FPMs demonstrated differences between its mechanism of action and that of CD on the actin cytoskeleton. Incremental additions of LA-B and mechanical measurements on FPMs were carried out serially as in the studies of CD. The data were averaged for at least three samples, and the same experiment was repeated at least twice. The concentration of LA-B needed to produce a significant effect on the tension and the stiffness of FPMs was much higher than that required of CD (Fig. 3D,E). This could be predicted from the dissociation constant measured in vitro for LA-A (~0.2 μM) (Coue et al., 1987). Force and stiffness had a sigmoidal dependence on LA-B concentration. The estimated half maximum concentrations for reducing the force and stiffness were 53 nM and 68 nM, respectively. The LA-B-dependent decrease of tension and stiffness was confined to a single decade of LA-B concentration, whereas the response to CD ranged over almost three decades. This strongly suggests that CD and LA-B operate by different mechanisms to disrupt the actin cytoskeleton.

We observe small differences in the values of force at the high concentration limits of CD and LA-B (Fig. 3). For example, the limiting value of the force at high CD concentration is ~10^{-4} N compared with an approximately 2-fold greater value for LA-B (Fig. 3A,C). Although this difference in force could have resulted from a small difference in the total extent of actin filament disruption by CD and LA-B, we think it more likely due to a larger relative contribution from the ECM in the latter measurements. Differences in the mechanical contributions of the ECM could result either from small differences in the extent of matrix remodeling during the formation of the FPMs or from small differences in the extent of stretching of the FPMs when they are mounted in the measuring instrument (Wakatsuki et al., 2000).

Table 1. Estimated half maximal dose of CD

	Dose without CS (μM)	Dose with CS (μM)
Force	0.25	0.25
Stiffness	0.25	0.25

The values are estimated from the curve (no curve fitting).

For a viscoelastic system the dynamic stiffness depends on both the elastic and viscous resistance to stretching. The viscous contribution can be measured by the phase angle, δ, between force and strain. In these experiments the change of phase angle due to disruption of the actin cytoskeleton was small (data not shown). Hence, CD and LA-B had a relatively minor effect on the viscosity of the tissues. Therefore, it is reasonable to suppose that the viscous contribution of the cells to FPM force and stiffness was also minor.

The effect of cell stimulation on the susceptibility to CD and LA-B

Stimulation of the cells in FPMs by calf serum (CS) influenced differently their responsiveness to CD and LA-B. Treatment of FPMs by CS (20% v/v) increased their tension and stiffness at least fivefold. This resulted primarily from activating myosin (Kolodney and Elson, 1993). The CS may also activate actin-binding proteins such as gelsolin to sever and cap actin

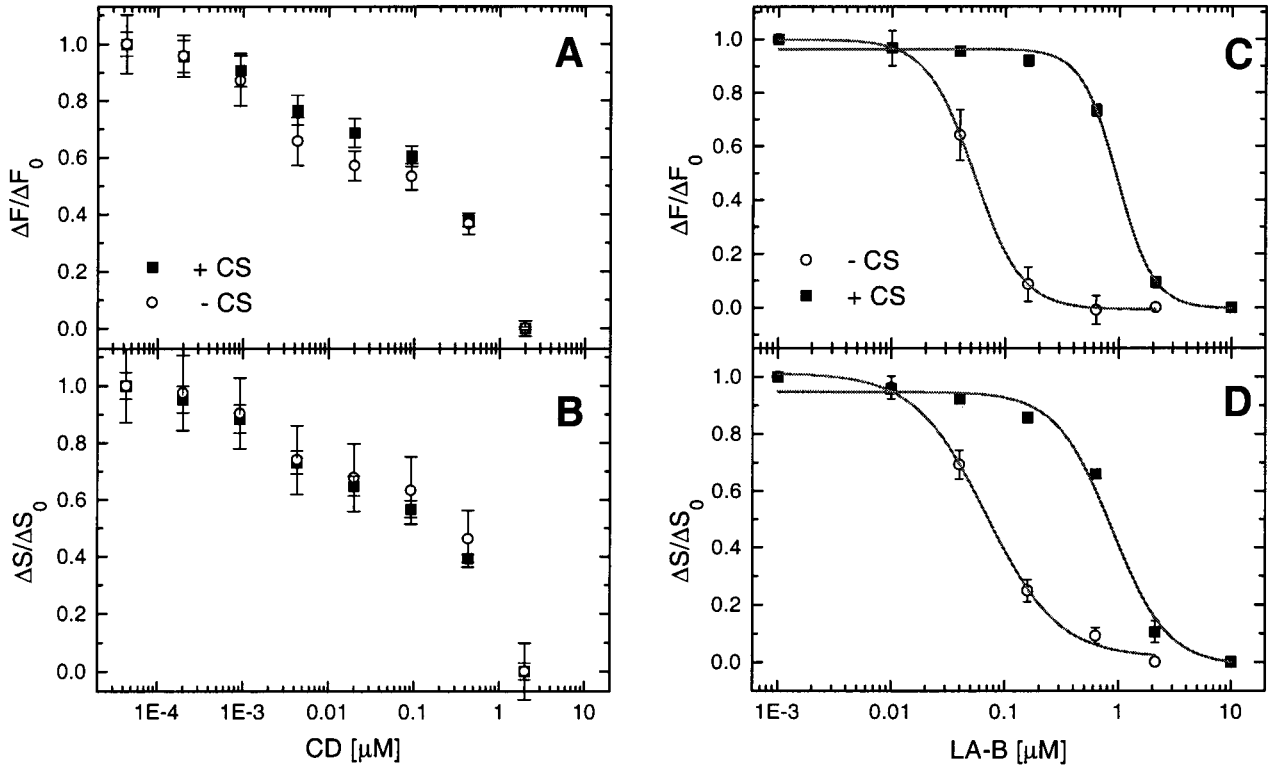

Fig. 4. Effect of CS on the sensitivity of force and stiffness to CD and LA-B. CS (20%) had no significant effect on sensitivity of force and stiffness to CD (A,B). In contrast, CS stabilized the actin cytoskeleton against LA-B. The concentration of LA-B required to disrupt the actin cytoskeleton is increased in the presence of CS (C,D).

filaments, or Arp2/3 to promote de novo actin polymerization. Fig. 4 illustrates the effects of CS on the sensitivity of FPMs to CD and LA-B. The tension and stiffness, normalized by their values prior to addition of CD or LA-B, are compared with data obtained without CS. CS did not significantly affect the sensitivity of the mechanical parameters to CD. In contrast, activation by CS shifted the response of FPMs to higher concentrations of LA-B, i.e. the addition of the CS decreased the susceptibility of the actin cytoskeleton to LA-B.

CD effects on single cells

Cell indentation measurements assess the effects of CD at the level of individual cells adherent to a substratum in monolayer culture. The CEFs were cultured on plastic coverslips (tissue culture grade) and indentation measurements were performed within 3 days. The cell stiffness was measured as resistance to indentation of the plasma membrane by a vertical glass probe tip of diameter about 2 μm as described briefly above. At each concentration of CD the indentation stiffness was measured on a number of cells before and 30 minutes after the CD treatment. The change in stiffness is shown in Fig. 5. There was a significant decrease in cell stiffness at and above 2 nM CD. The effects of CD on the stiffness were similar for both the indentation measurements on single cells and the measurements on FPMs over a wide range of concentrations. The stiffness did not change significantly (P=0.05) by DMSO alone (result not shown).

Simulating the CD and LA-B effects

Our quantitative measurements have shown that the concentration of CD required for half maximal disruption of the actin cytoskeleton is in the range of ~0.25 μM. This is two orders of magnitude higher than the dissociation constant measured on purified actin filaments (~2 nM). A simple model in which CD and actin-capping proteins compete for binding to the barbed ends of actin filaments illustrates one mechanism that can explain this discrepancy. We suppose that to be

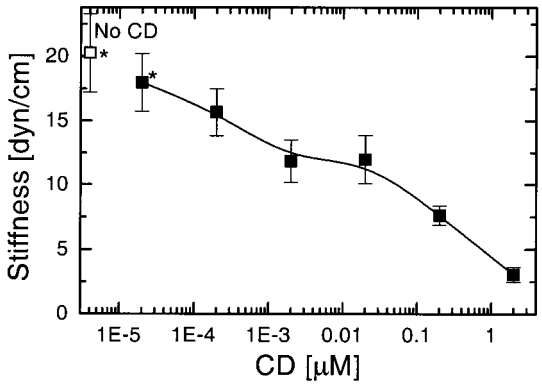

Fig. 5. Indentation stiffness. The CEFs were cultured on coverslips and indentation measurements were performed. Resistance to indentation by a glass micro probe was measured as described in Materials and Methods. At each concentration of CD the indentation stiffness was measured on a population of cells before and 30 minutes after treatment with each CD concentration. There was a significant decrease in the stiffness of the cells at and above 2 nM CD. *The two means were not significantly different (P=0.05).

mechanically effective, actin filaments must be anchored to the cell membrane and must transmit tension through the membrane to the extracellular matrix or to neighboring cells. For the filaments to remain stable within the cytoplasm, capping proteins must block their barbed ends. Both ERM family proteins and tensin cap the barbed ends of actin filaments and closely associate with cell/cell or cell/matrix contact sites (Lo et al., 1994b; Shuster and Herman, 1995; Shuster et al., 1996; Vaheri et al., 1997). CapZ also associates with the barbed ends of actin filaments and may indirectly anchor them to these sites. CD disrupts this anchorage by displacing the capping protein without depolymerizing actin filaments. Retraction of actin filaments displaced from their anchorage by 2 μM CD into large focal aggregates (Fig. 1H) is most likely driven by the myosin activity as previously shown by Verhkovsky et al. (Verkhovsky et al., 1997). Active myosin retracts stable actin filaments detached from capping proteins but capped by CD. At lower CD concentrations, fewer filaments are displaced and retracted. Therefore, we propose that CD influences cell mechanical properties by competing with barbed end capping proteins that stabilize actin filaments and/or anchor them to the membrane. A simple mathematical scheme was constructed to represent this model, which is described by the following five reactions (1-5) and three conservation conditions (6-8):

$$n \cdot A \leftrightarrow E \quad (1)$$

$$E + P \leftrightarrow EP \quad (2)$$

$$E + C \leftrightarrow EC \quad (3)$$

$$C + 2A \leftrightarrow CA_2 \quad (4)$$

$$A + B \leftrightarrow AB \quad (5)$$

$$[A_T] = n([E] + [EP] + [EC]) + 2[CA_2] + [AB] + [A] \quad (6)$$

$$[P_T] = [P] + [EP] \quad (7)$$

$$[B_T] = [B] + [AB] \quad (8)$$

Here, $\leftrightarrow$ denotes a chemical equilibrium. A,E,P,B and C represent actin monomer, an actin filament with exposed barbed end, an unoccupied barbed end capping protein (bound directly or indirectly to the cell membrane), an unoccupied actin monomer binding protein, and CD, respectively. Reaction (1) is a polymerization equilibrium between the actin monomer, A, and the n-mer actin filament, E. For this simple model we have defined an effective dissociation constant for actin polymerization, Kn, which accounts for both nucleation and elongation phases as shown in the Appendix (Equation 26). We take n, the number of actin monomers in an actin filament of average length, ~500 nm, to be 200 (Alberts et al., 1994). Reaction (2) describes the binding of a capping protein molecule to the barbed end of an actin filament. Once a capping protein is bound to the actin filament, polymerization is halted (as we are neglecting addition of monomers to the pointed end). Although there could be many species of capping proteins in fibroblasts, we consider, for illustrative purposes, a simple competitive binding of only one species. The capped filaments are anchored to membrane and can thereby directly or indirectly to transmit forces to the extracellular matrix or substratum. We suppose that this anchorage is necessary for actin filaments to influence cellular mechanical properties. Reaction (3) represents CD binding

Table 2. Dissociation constants and conservation molecules

(a) Dissociation constants related to the actin polymerization		
Dissociation constants	Value (μM)	Reference
Actin nucleation (n<4)		
$L_1=[A]\,[A]/[A_2]$	100,000	(Pollard and Cooper, 1986)
$L_2=[A_2]\,[A]/[A_3]$	100,000	(Pollard and Cooper, 1986)
ATP-actin polymerization		
$K=[A_{n-1}]\,[A]/[An]$	0.1	(Carlier, 1998)
Capping protein and F-actin barbed end		
$K_P=[P]\,[E]/[PE]$	0.01*	(Carlier, 1998)
Thymosin β_4 and actin monomer		
$K_{BT}=[A]\,[B]/[AB]$	1	(Goldschmidt-Clermont et al., 1992)
(b) Conservation of the molecules		
Molecules	Value (μM)	Reference
Total actin (A_T)	100	(Alberts et al., 1994)
Total capping protein (P_T)	1	(Carlier, 1998)
Total thymosin β_4 (B_T)	500	(Carlier and Pantaloni, 1997)
(c) Dissociation constants of the reagents		
Dissociation constants	Value (μM)	Reference
CD and barbed end F-actin		
$K_C=[C]\,[E]/[CE]$	0.002	(Cooper, 1987)
CD and actin monomers		
$K_{C1}=[C]\,[A]/[CA]$	2.5	(Goddette and Frieden, 1986)
$K_{C2}=[CA]\,[A]/[CA_2]$	0.5	(Goddette and Frieden, 1986)
$K_2=K_{C1}\,K_{C2}=[C]\,[A]^2/[CA_2]$	1.25	(Goddette and Frieden, 1986)
LA-B and actin monomers		
$K_L=[L]\,[A]/[LA]$	0.2	(Coue et al., 1987)

*The value is chosen from a range (0.001~0.01).

to the barbed end of actin filaments in competition with the capping protein. CD binds not only the barbed end of polymeric filaments but also to two actin monomers to make the dimer complex, AC_2 (Reaction (4)) (Goddette and Frieden, 1986). This monomer sequestering effect can be ignored at low but not at high concentrations of CD. We have also accounted for the sequestering of actin monomer by binding to proteins such as thymosin β_4 and profilin. Since the former is thought to dominate this process (Goldschmidt-Clermont et al., 1992), we have included a single monomer binding reaction (Reaction (5)). The rest of the equations describe the conservation of the total actin (A_T), total capping protein (P_T) and the total thymosin β_4 (B_T), where the square brackets denote the concentration of the molecule in the cell. We have assumed the nucleotide bound to free actin monomer is ATP, owing to the catalytic effect of profilin on nucleotide exchange (Goldschmidt-Clermont et al., 1992). We have also assumed that [C] is always equal to the CD concentration in the medium surrounding the FPM. These equations were solved analytically to yield [EP] (see Appendix), which we assumed to be linearly correlated with the force and stiffness of the FPM. Curves depicting the concentration dependence of the mechanical response were generated using published values of dissociation constants shown in Table 2a-c. Each panel of Fig. 6A-F has a curve calculated using the values listed in Table 2 and two other curves calculated using two different values of a specific parameter. The results were substantially sensitive only to the total concentration of capping protein, P_T, and the dissociation constant for its binding to actin filaments, K_P.

The tighter the binding of the capping protein to actin, the higher the concentration of CD needed for competitive binding and therefore disruption of the actin cytoskeleton (Fig. 7A). As expected, increasing the amount of the capping protein or its affinity for actin filaments had similar effects (Fig. 7B). Although changing the critical concentration (K, effectively, the dissociation constant of the actin monomer from the barbed end of the filament), total thymosin-β_4 (B_T) and effective length of actin filaments (n) had an effect on the total concentration of the capped filaments, there was almost no effect on the shapes of the normalized curves or their positions on the CD concentration axis. Also, changing the dissociation constant of the CD-actin dimer complex, K_2 had no perceptible effect on the calculated curves. Although our assumption that the fractional change of force and stiffness is proportional to the fractional change in the actin filaments bound to capping proteins may not be valid in detail, it provides a reasonable starting point for this mechanistic illustration.

The dissociation constant of LA-B in vitro is 0.2 μM, fourfold greater than the concentration of LA-B that causes a half-maximal decrease in FPM mechanical parameters (0.05-0.07 μM for FPMs in the absence of added CS, Table 3). The significant increase caused by calf serum of the concentration of LA-B required to disrupt actin in cells suggests that serum stimulates processes which stabilize actin filaments. A model similar to that used for CD was constructed to explain the effect of LA-B on the mechanical properties of FPMs. The model is described by the following four reactions (9-12) and three (13-15) conservation conditions:

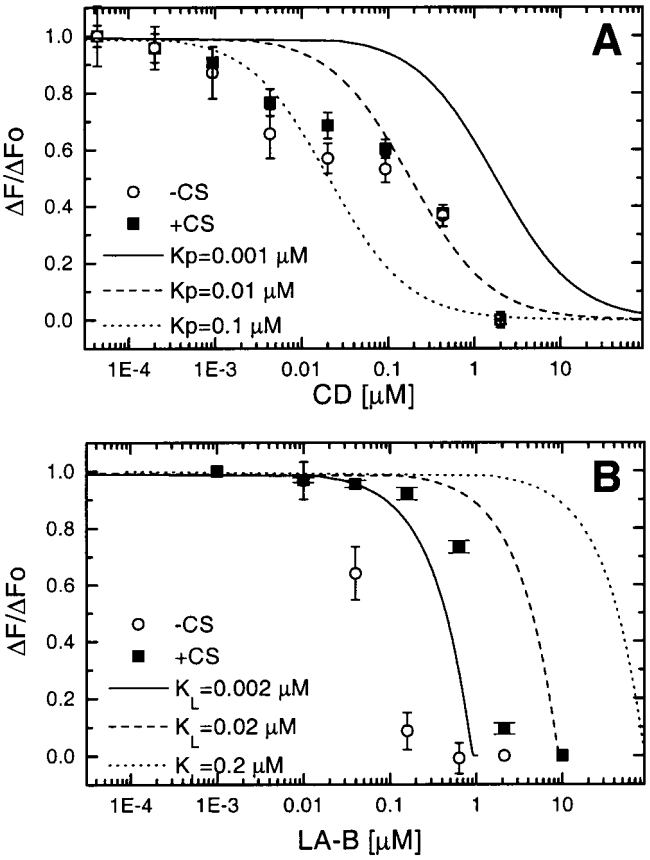

Fig. 6. Comparison of experiments and simulations. The percent changes in force at various concentrations of CD and LA-B were compared to the corresponding simulations. Using 10-100 nM for K_P best simulates the CD concentration dependent curves (A). Nevertheless, the experimental data exhibited effects on force and stiffness over a still wider range of CD concentration. The LA-B curves simulated the narrow range of LA-B concentrations affecting the mechanical properties of the FPMs (B).

$$nA \leftrightarrow E \tag{9}$$

$$E + P \leftrightarrow EP \tag{10}$$

$$L + A \leftrightarrow LA \tag{11}$$

$$A + B \leftrightarrow AB \tag{12}$$

$$[A_T] = n \cdot ([E] + [EP]) + [LA] + [AB] + [A] \tag{13}$$

$$[P_T] = [P] + [EP] \tag{14}$$

$$[B_T] = [B] + [AB] \tag{15}$$

Reactions 9, 10 and 12 are the same as reactions 1, 2 and 4 of the CD model. As before, we assume that the tension and stiffness are linearly proportional to the concentration of EP. According to this model, binding of actin monomer by LA-B inhibits the polymerization of actin filaments, as described in reaction (9). Reactions 13-15 account for the conservation of the total actin, total capping protein, and thymosin β_4. The concentration of the LA-B is assumed to be always equal to the concentration of the drug in the medium surrounding the FPM.

The variation with LA-B concentration of the fraction of capping protein bound to the barbed ends of actin filaments is shown in Fig. 7G-L. As for CD, each panel has a curve calculated using the values listed in Table 2 and two other curves plotted using two different values of a specific parameter. In contrast to the CD model, the calculated plots were relatively insensitive to the total amount of capping protein and the affinity of the capping protein for actin filaments. The results are sensitive to the value of the critical constant (K), the total amount of monomer sequestering protein (B_T), the dissociation constant for binding of actin monomer to LA-B (K_L) and, to a lesser extent, the effective degree of polymerization of the actin filaments (n).

Model and the data

The most striking difference in the effects of CD and LA-B on the mechanical properties of FPMs was the range of concentrations over which the two compounds acted. Although the mechanical parameters were very sensitive even to small concentrations of CD (<1 nM), the maximum disruptive effect on the actin cytoskeleton required a high concentration (~2 μM) of CD. LA-B, however, had a smaller range of effective concentrations, typically only one decade in a log-scale plot. Fig. 6 compares the data and the simulated curves generated by the models with the parameter values listed in Table 2. The model simulation partially reproduced the observed wide range of effective concentrations of CD (Fig. 6A). Nevertheless, the simulation still had a smaller effective concentration range than the experimental measurements. We could simulate the wider effective concentration range seen experimentally by including two species of capping proteins with different dissociation constant values. Hence, the data suggest the existence of different kinds of capping proteins with different dissociation constants for filament ends.

The simulated curves using the parameter values listed in Table 2, including the dissociation constant, K_L, of the LA-A complex (0.2 μM), did not match the experimental data. The range of effective LA concentration simulated by taking K_L=0.2 μM was too high. Lowering K_L yielded a closer fit to the data (Fig. 6B). This could be due to the different

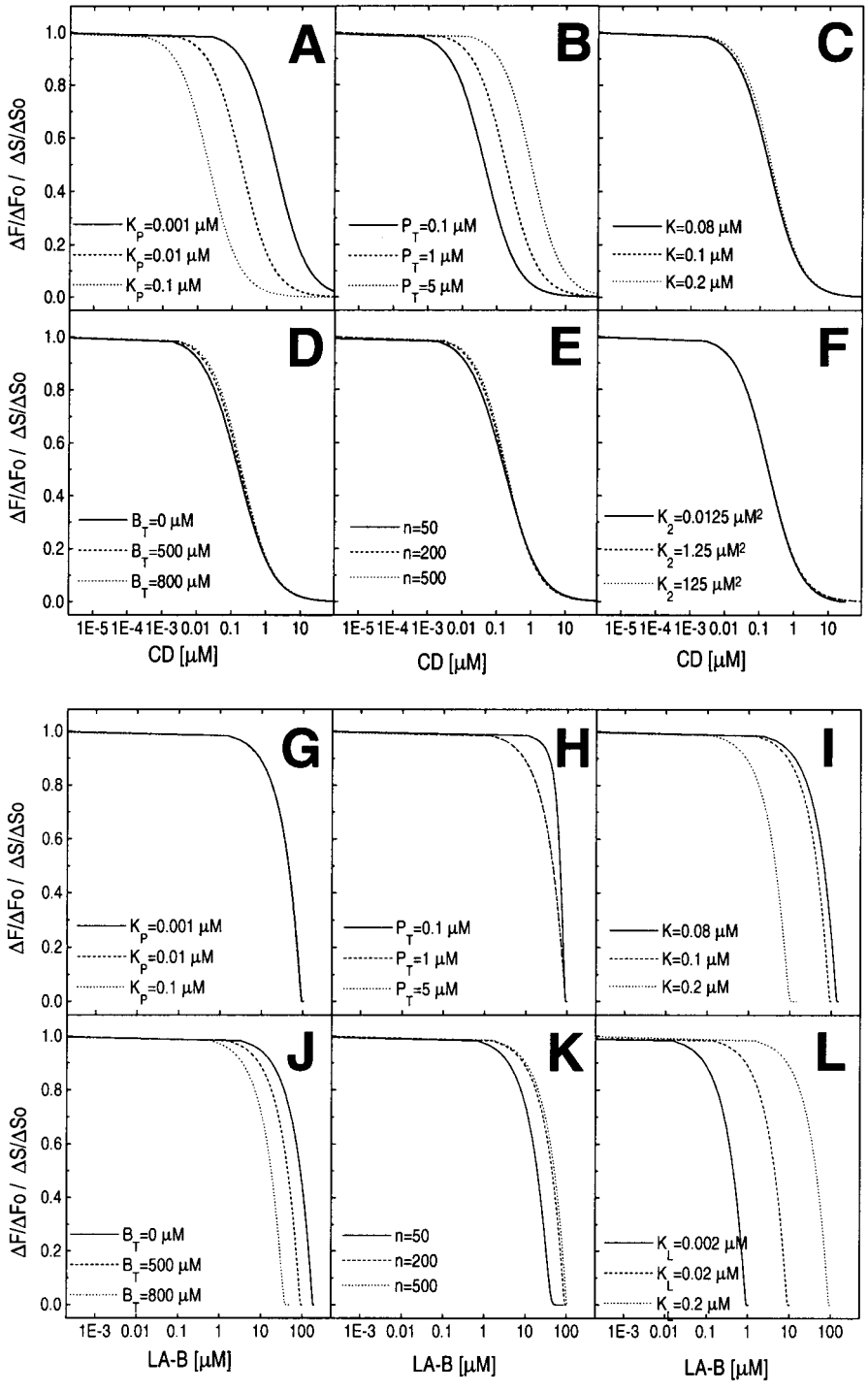

Fig. 7. Simulation of the dependence of force and stiffness on the concentrations of CD and LA-B. Sensitivity of the models for CD and LA-B effects on force and stiffness. Each of the parameters in (Equation 25) was varied individually. Both decreasing K_P, i.e. strengthening capping protein binding (A) and increasing total amount of capping protein, P_T, (B) shifts the effective range of CD to higher concentrations. Changing the critical concentration for polymerization, K, (C), the concentration of total actin monomer binding protein, B_T (D), the average actin filament length, n, (E) and the dissociation constant of the actin monomers to CD, K_2, (F) all had negligible effects on the CD concentration dependence of computed force and stiffness, i.e. [EP]. Conversely, a similar analysis using Equation 26 to estimate the effects of LA-B demonstrates that [EP] is sensitive to the critical constant, K, (I), the concentration of total monomer binding protein, B_T, (J), the dissociation constant for LA-B, K_L, (L), but no other parameters (G,H,K).

Table 3. Estimated half maximal dose of LA-B

	Dose without CS (μM)	Dose with CS (μM)
Force	0.053±0.001	0.096±0.076
Stiffness	0.068±0.007	0.087±0.161

The value are estimated by fitting a sigmoidal function to the data.
The errors are standard deviations estimated by the fitting.

biochemical environment in cells compared to the binding assay conducted in vitro (Coue et al., 1987) or to some complex interaction of LA-B with other molecules in cells.

DISCUSSION

Actin polymer network and cell mechanics

We have measured the mechanical properties of fibroblasts to assay the state of their actin cytoskeletons. It has long been known that disruption of the cytoskeleton causes a dramatic reduction of cell stiffness (e.g. Petersen et al., 1982). Actin filaments help to distribute and support contractile stresses generated within a cell as well as external stresses transmitted among cells either directly or through the ECM. This requires that the filaments be anchored to large, stable structures within the cell, especially the plasma membrane. Therefore, we propose as a working hypothesis that actin filaments are both stabilized and perhaps anchored in the plasma membrane by barbed end capping proteins. The morphological and mechanical consequences of CD would then result from its competitive binding to the barbed ends of actin filaments, thereby destabilizing and displacing them from their sites of anchorage. This hypothesis explains both the effects of CD on cell mechanical properties and their CD concentration dependence.

Do our measurements on FPMs characterize changes in the mechanical properties of the cells that they contain? In general the stresses that the cells sustain in a FPM depend on the mechanical characteristics not only of the cells but also of the ECM (Zahalak et al., 2000). CD and LA-B have no direct effect on collagen gels prepared without cells (data not shown). Because actin filaments are connected through the plasma membrane to the ECM via integrins, however, it is possible that disruption of the actin cytoskeleton also has an effect on the mechanical properties of the ECM. For illustrative purposes, we suppose that, if disruption of the actin cytoskeleton does perturb the ECM, then the mechanical properties of both the cells and the matrix change correspondingly. This is to be expected if the effects of the cells on the ECM result mainly from interactions with the actin cytoskeleton. Supporting this hypothesis is the observation that the dependence on CD concentration of cell stiffness measured by indentation (Fig. 5) is qualitatively similar to that observed for FPMs even though the former measurements were carried out on individual cells in monolayers and in the absence of large amounts of ECM. More detailed experimental and theoretical analyses are required to test the accuracy of this approximation, but it is sufficient for our present purposes. Therefore, we have assumed that the displacement by CD of actin filaments from their barbed-end anchorage accounts for the mechanical changes observed in FPMs at different CD concentrations.

Our results demonstrate that cell contractile force measured in FPMs or cell stiffness, measured either by indentation of single cells or by strain-induced force in FPMs, provide a sensitive indicator of the physical state of the actin cytoskeleton. From these measurements, we conclude that significant changes of cellular mechanical properties are observed at very low CD concentrations (2 nM), which cause changes in the organization of the actin cytoskeleton that are so slight as to be undetectable by fluorescence microscopy. The effects of CD and LA-A on the stiffness of single cells adherent to a rigid substratum have been investigated using AFM (Rotsch and Radmacher, 2000). Although a reduction in stiffness was observed for high concentrations of CD, effects on stiffness were undetectable by AFM for CD concentrations less than 2 μM. In contrast, a reduction in stiffness of cells in the presence of 10% serum was observed by AFM for a LA-A concentration of 0.1 μM, tenfold lower than the concentration range over which force and stiffness decreased in FPMs. Hence, it appears that mechanical effects of CD are detectable much more sensitively in FPM measurements and by our indentation measurements, which used a relatively larger indenter area and indentation depths, than by AFM. The reverse order of sensitivity to the effects of Latrunculin might indicate that the binding affinity for actin monomer in cells is greater for LA-A than for LA-B or that actin filaments in CEF in FPMs are less sensitive to LA than are 3T3 or NRK cells in monolayer culture.

Effective concentrations of CD and LA-B in vitro and in vivo

A striking difference between CD and LA-B in their effects on the mechanical properties of FPMs is the range of concentrations over which the two compounds act. Although the mechanical parameters are sensitive even to nanomolar concentrations of CD, maximal cytoskeletal disruption requires concentrations in the micromolar range. In contrast, LA-B, is effective over a smaller concentration range, spanning approximately one decade. Fig. 6 compares the experimental data with the results of simulation using the parameter values listed in Table 2.

The proposed competitive binding hypothesis accounts for the striking 2-3 order of magnitude discrepancy between the binding of CD to isolated actin filaments (~2 nM) and the concentration range over which the major effects on both cell morphology and mechanical properties of cells and tissue models (0.2-2 μM) are observed. The higher the affinity of the capping proteins for barbed filament ends, the higher the concentration of CD needed to compete with and displace these filaments from their sites of anchorage. This idea is put into more quantitative form in equations 1-8 above. As expected, the most sensitive parameters of the model were the dissociation constant for binding the capping protein to the F-actin barbed ends and the total capping protein concentration. Using the published parameters listed in Table 2, this model yields a reasonable fit to the experimental data (Fig. 6A). The model illustrates that CD has a significant effect on cell mechanical properties over a relatively wide (100-fold) concentration range. For example, for the curve calculated for K_P=0.01 μM (which best fits the major disruption of cytoskeletal morphology and mechanical properties), $\Delta F/\Delta F_0$ varies from 0.9 to 0.1 as CD varies from 0.02 μM to 2.0 μM. Nevertheless, the actual range of CD concentrations over which perceptible effects on cellular mechanics are observed is even wider. The noticeable decrease in $\Delta F/\Delta F_0$ for CD concentrations even in the range ~1 nM suggests the existence of a population of filaments bound to anchorage sites of low affinity that are readily displaced by CD.

Fig. 6A suggests that there are at least two classes of filament binding sites, a smaller population and a larger population with dissociation constants in the range of ~1 μM and 10 nM, respectively. The former could include βCAP73 and the latter, tensin, as ezrin-associated βCAP73 completely dissociates from the barbed ends of actin filaments at 10 nM of CD (Shuster et al., 1996) and the Kd of tensin is ~20 nM (Lo et al., 1994b).

The formation of complexes between CD and an actin dimer has been observed in the μM range of CD concentrations (Goddette and Frieden, 1986). CD could sequester G-actin and inhibit actin polymerization at this higher concentration. Even a 100-fold decrease in the combined dissociation constant of the complex, K_2, however, did not influence the simulated curves (Fig. 7F). This reinforces our conclusion that the strong affinity of CD for the barbed ends of actin filaments is responsible for the primary effect on the mechanical properties of cells.

In vitro experiments suggest that cytochalasin B at high concentration (30 μM) might also sever actin filaments (Theodoropoulos et al., 1994). We cannot now assess the contribution of this mechanism in our experiments. We note, however, that displacement of an actin filament from a capping protein by CD is formally similar to creation of a new CD-capped barbed end at an interior site of an actin filament, as would occur if severing by CD occurred. Hence, our illustrative model would also be applicable with minor modifications to a severing mechanism.

The concentration of Latrunculin commonly used to disrupt F-actin in cells (Spector et al., 1989), is in the same range as the dissociation constant for binding of LA-A to the actin monomer as measured in vitro (Coue et al., 1987) (Kd=0.2 μM). The concentration of LA-B required for half-maximal disruption of cellular mechanical properties estimated from our experiments was ~60 nM and ~900 nM in the absence and presence of CS, respectively. (Table 3). In contrast, the half-maximal concentration of LA-B estimated from the simulation (equations 9-15), using the in vitro dissociation constant of LA-A was ~45 nM.

The simulation is very sensitive to at least two parameters, the dissociation constant (K_L) of LA-B for monomer actin and the critical concentration (K) for actin polymerization. We have assigned the critical concentration the value 0.1 μM (Table 2a). Then setting a value of K_L=~0.004 μM brings the simulation into agreement with the experimental observations. We can also bring the simulation into agreement with the force and stiffness measurements by increasing the critical concentration to 0.235 μM and assigning K_L=0.2 μM (Coue et al., 1987). (Note that the critical G-actin concentration measured by Coue et al., is 0.24 μM, but the effects on the simulated results of changing the value of K_L from 0.1 μM to 0.24 μM are inconsequential.) Therefore, the discrepancy between the simulated and experimental data for LA-B might be due either to differences between the stability of the complexes of LA-B and LA-A with actin or to differences between the critical concentration for actin polymerization in a test tube and in cytoplasm. More complete measurements of the binding constants of LA-A and LA-B with actin and of the critical concentration of actin in cells are needed to resolve this question.

Cellular viscosity

Measurements of the phase angle indicate that the contribution of cellular viscosity to the overall tissue viscosity were small in these experiments. The observed changes of phase angle in response both to CD and LA-B coincided with the major disruption of cytoskeletal actin. Although stiffness and force decreased by almost twofold at CD concentrations below 0.1 μM, the phase angle decreased significantly only for CD > 0.1 μM, coinciding with major changes in the actin cytoskeleton observable by fluorescence microscopy (data not shown). It is likely that the meshwork of actin filaments contributes to cellular viscosity by impeding the flow of cytoplasm during cellular deformation. Detached filaments that remained entangled within the actin filament meshwork could continue to contribute to cytoplasmic viscosity, even after their contribution to cellular force and stiffness had been eliminated.

The effect of calf serum

Calf serum has no significant effect on the sensitivity of cell tension and stiffness to CD (Fig. 4A). In contrast CS displaces the effect of LA-B on both $\Delta F/\Delta F_0$ and $\Delta S/\Delta S_0$ to higher LA-B concentrations, effectively stabilizing the actin cytoskeleton against the action of LA-B. This could be explained by supposing that CS substantially increases the stability of actin filaments either by decreasing the affinity of actin monomer-binding proteins or by effectively decreasing the critical concentration for actin polymerization, e.g., by enhancing filament nucleation. As shown in Fig. 6, our model predicts that neither the extent of monomer sequestration, represented by B_T, nor the critical concentration for polymerization (K) has a substantial effect on the variation of FPM mechanical properties with CD concentration. In contrast, the dependence of the mechanical properties on the concentration of LA-B is sensitive to both B_T and K (Fig. 7). Hence, as observed in our experiments, our models predict that the action of LA-B but not CD would be sensitive to an effect of CS on the stability of actin filaments. Corroborating this interpretation are observations that lysophosphatidic acid (LPA), an active component of CS, enhances actin polymerization in MMI tumor cells (Mukai et al., 1999). We would not, however, expect the effect of CS to be mediated by stabilizing the interaction of capping proteins with actin filaments because, according to our model, this would have a substantial effect on the sensitivity of FPMs to CD.

Another important contribution of CS to the stability of the actin cytoskeleton could occur via activation of myosin II (cf. Kolodney and Elson, 1993). LPA is an activator of myosin via the GTP binding protein, Rho (Hall, 1998). Moreover, it has been shown that inactivation of myosin in fibroblasts by specific antibodies caused a disruption of stress fibers (Honer and Jockusch, 1988), and, conversely, activation of myosin enhances stress fiber formation (Chrzanowska-Wodnicka and Burridge, 1996). Crosslinking of actin filaments not only in stress fibers but also within an actin meshwork could stabilize the filaments.

In summary, the simplest interpretation of the effect of CS on the sensitivity of the actin cytoskeleton to CD and LA-B is that CS stabilizes actin filaments but does not enhance their capping at barbed ends. Our simulations demonstrate that this is consistent with the strong effect of CS on the sensitivity to LA-B and its undetectable effect on the sensitivity to CD. Other factors such as activation of myosin and elevation of cytoplasmic calcium ion concentration, which are also known to occur in response to CS, could also play a role in modulating the sensitivity to LA-B.

Mechanical properties of cells and tissue models as indicators of cytoskeletal structure

This work demonstrates that measurements of the mechanical properties either of cell populations in reconstituted model tissues or of individual cells in monolayer culture can provide sensitive and quantitative indicators of the structure and mechanical function of the cytoskeleton. Up to now the effects of cytoskeletal perturbants such as CD and LA have been evaluated mainly through qualitative observations of cytoskeletal morphology. In this work we could compare measurements of the force exerted by and the stiffness of FPMs with quantitative molecular binding models of the mechanism of action of CD and LA-B. This approach is likely to be useful in the future to provide a readout of the mechanical functions of natural cytoskeletal components such as filament capping, severing and crosslinking proteins.

We have shown a close correspondence between the effects of CD on the mechanical properties of individual cells in monolayer cultures (Fig. 5) and on a population of cells in a reconstituted tissue model (Fig. 3). An advantage of the tissue model is that it provides the averaged response of a large population of cells. A large number of indentation measurements on individual cells are required to obtain a statistically representative characterization of a monolayer population. Nevertheless, the indentation measurements offer the potential advantage of a close comparison of the mechanical measurement with simultaneous microscopic observation of the cell being probed. The interpretation of measurements both of individual cells and reconstituted tissues would be substantially enhanced by quantitative theoretical models that related the measured properties to the mechanical characteristics, structure, and organization of the cytoskeletal and extracellular matrix constituents of the cells and tissue models.

APPENDIX

Simulation of the dependence of cellular mechanical properties on the concentration of CD (derivation)

The steady state concentration ratios for reactions 1-5 can be written using the dissociation constants listed in Table 2 (Equations 16-20).

$$K = \frac{[A_{n-1}]\cdot[A]}{[A_n]}, \tag{16}$$

$$K_P = \frac{[E][P]}{[EP]}, \tag{17}$$

$$K_C = \frac{[E][C]}{[CE]}, \tag{18}$$

$$K_2 = \frac{[C][A]^2}{[CA_2]}, \tag{19}$$

$$K_{B_T} = \frac{[A][B]}{[AB]}, \tag{20}$$

From Equations 17 and conservation condition 7 we can deduce that (Equation 21)

$$[E] = \frac{K_P[EP]}{[P_T]-[EP]}. \tag{21}$$

From Equation 20 and conservation condition 8 we obtain (Equation 22),

$$[AB] = \frac{[B_T]}{K_{B_T}/[A]+1}. \tag{22}$$

[EC] and [CA_2] are obtained by solving Equations 18 and 19, respectively, and are substituted into Equation 6, which, together with Equation 22 yields,

$$[A_T] = n([E]+[EP]) + [C]\left\{\frac{n[E]}{K_C} + \frac{2[A]^2}{K_2}\right\} + \frac{[B_T]}{K_{B_T}/[A]+1} + [A], \tag{23}$$

where

$$[A] = ([E]Kn)^{1/n}. \tag{24}$$

Using Equation 22 and Equation 24, Equation 23 was reduced to an equation containing only two unknown variables, [EP] and [C]. (The other parameters are provided as constants in Table 2.) Since the change in [EP] with variation of [C] is to be simulated, it is natural to solve Equation 23 for [EP] in terms of [C]. This, however, entails obtaining roots of an (1/n)th power polynomial. A simpler approach is to compute values of [C] for an appropriate range of values of [EP]. The results can then be replotted to provide the desired dependence of [EP] on [C]. Therefore, Equation 23 was solved for [C] (Equation 25):

$$[C] = \frac{1}{\dfrac{n[E]}{K_C} + \dfrac{2[A]^2}{K_2}}\left\{[A_T] - n([E]+[EP]) - \frac{[B_T]}{K_{B_T}/[A]+1} - [A],\right\}, \tag{25}$$

where [E] and [A] are given by Equations 21 and 24, respectively.

A similar approach was used to obtain the dependence of [EP] on the concentration of LA-B, [L]. Analogous to Equation 25, we obtained an equation from which to calculate the concentration [L] in terms of [EP] (Equation 26).

$$[L] = \frac{K_L}{[A]}\left\{[A_T] - n([E]+[EP]) - \frac{[B_T]}{K_{B_T}/[A]+1} - [A]\right\}. \tag{26}$$

Value for Kn

The dissociation constant for the actin polymerization, Kn, was obtained by combining the nucleation and chain elongation processes. Therefore, Kn becomes a product of each actin monomer binding to the filament described as (Equation 27):

$$Kn = L_1 \cdot L_2 \cdot L_3 \cdot \ldots L_{n-1}. \tag{27}$$

Except for the nucleation steps (L_1 and L_2), the dissociation constants of the subsequent monomer binding reactions were all equal to the critical concentration of ATP-bound actin monomer binding to the barbed end of actin filaments, K. Thus, the value of $(Kn)^{1/n}$ used in Equation 24 was calculated by Equation 28:

$$(Kn)^{1/n} = \frac{(L_1L_2)^{1/n}K}{K^{3/n}}. \tag{28}$$

Dissociation constant of actin polymerization

The critical concentration for addition of monomers to the barbed ends of actin filaments is lower by almost tenfold than that for addition at the pointed end (Pollard and Cooper, 1986). Hence, the effective critical concentration overall should be close to that for the barbed ends. In our simulations we use the steady-state ATP-bound actin monomer concentration, C_{SS}, as the dissociation constant, K, (i.e. critical G-actin concentration). For simplicity, we ignore the distinction between the monomer dissociation constants at the barbed and pointed filament ends. In addition C_{SS} is the actin monomer concentration relevant for binding to G-actin binding proteins and to LA-B. Following Carlier et al., we have set C_{SS}=0.1 (Carlier, 1998).

This work was supported by a NIH grant to E.L.E.

REFERENCES

Alberts, B., Bray, D., Lewis, J., Raff, M., Roberts, K. and Watson, J. D. (1994). *Molecular Biology of the Cell*. New York: Garland Publishing.

Carlier, M. F. (1998). Control of actin dynamics. *Curr. Opin. Cell Biol.* **10**, 45-51.

Carlier, M. F. and Pantaloni, D. (1997). Control of actin dynamics in cell motility. *J. Mol. Biol.* **269**, 459-467.

Chrzanowska-Wodnicka, M. and Burridge, K. (1996). Rho-stimulated contractility drives the formation of stress fibers and focal adhesions. *J. Cell Biol.* **133**, 1403-1415.

Cooper, J. A. (1987). Effects of cytochalasin and phalloidin on actin. *J. Cell Biol.* **105**, 1473-1478.

Coue, M., Brenner, S. L., Spector, I. and Korn, E. D. (1987). Inhibition of actin polymerization by latrunculin A. *FEBS Lett* **213**, 316-318.

Elson, E. L. (1988). Cellular mechanics as an indicator of cytoskeletal structure and function. *Annu. Rev. Biophys. Biol. Chem.* **17**, 397-430.

Elson, E. L., Felder, S. F., Jay, P. Y., Kolodney, M. S. and C, P. (1996). Forces and Mechanical Properties in Cell Locomotion. In *Motion Analysis of Living Cells* (ed. D. Soll). New York: John Wiley.

Elson, E. L., Pasternak, C., Daily, B., Young, J. I. and McConnaughey, W. B. (1984). Cross-linking surface immunoglobulin increases the stiffness of lymphocytes. *Mol. Immunol.* **21**, 1253-1257.

Goddette, D. W. and Frieden, C. (1986). The kinetics of cytochalasin D binding to monomeric actin. *J. Biol. Chem.* **261**, 15970-15973.

Goldschmidt-Clermont, P. J., Furman, M. I., Wachsstock, D., Safer, D., Nachmias, V. T. and Pollard, T. D. (1992). The control of actin nucleotide exchange by thymosin beta 4 and profilin. A potential regulatory mechanism for actin polymerization in cells. *Mol. Biol. Cell* **3**, 1015-1024.

Hall, A. (1998). Rho GTPases and the actin cytoskeleton. *Science* **279**, 509-514.

Honer, B. and Jockusch, B. M. (1988). Stress fiber dynamics as probed by antibodies against myosin. *Eur. J. Cell Biol.* **47**, 14-21.

Janmey, P. A., Euteneuer, U., Traub, P. and Schliwa, M. (1991). Viscoelastic properties of vimentin compared with other filamentous biopolymer networks. *J. Cell Biol.* **113**, 155-160.

Janmey, P. A., Hvidt, S., Kas, J., Lerche, D., Maggs, A., Sackmann, E., Schliwa, M. and Stossel, T. P. (1994). The mechanical properties of actin gels. Elastic modulus and filament motions. *J. Biol. Chem.* **269**, 32503-32513.

Kojima, H., Ishijima, A. and Yanagida, T. (1994). Direct measurement of stiffness of single actin filaments with and without tropomyosin by in vitro nanomanipulation. *Proc. Natl. Acad. Sci. USA* **91**, 12962-12966.

Kolodney, M. S. and Elson, E. L. (1993). Correlation of myosin light chain phosphorylation with isometric contraction of fibroblasts. *J. Biol. Chem.* **268**, 23850-23855.

Kolodney, M. S. and Wysolmerski, R. B. (1992). Isometric contraction by fibroblasts and endothelial cells in tissue culture: a quantitative study. *J. Cell Biol.* **117**, 73-82.

Lo, S. H., An, Q., Bao, S., Wong, W. K., Liu, Y., Janmey, P. A., Hartwig, J. H. and Chen, L. B. (1994a). Molecular cloning of chick cardiac muscle tensin. Full-length cDNA sequence, expression, and characterization. *J. Biol. Chem.* **269**, 22310-22319.

Lo, S. H., Janmey, P. A., Hartwig, J. H. and Chen, L. B. (1994b). Interactions of tensin with actin and identification of its three distinct actin-binding domains. *J. Cell Biol.* **125**, 1067-1075.

Mukai, M., Imamura, F., Ayaki, M., Shinkai, K., Iwasaki, T., Murakami-Murofushi, K., Murofushi, H., Kobayashi, S., Yamamoto, T., Nakamura, H. et al. (1999). Inhibition of tumor invasion and metastasis by a novel lysophosphatidic acid (cyclic LPA). *Int. J. Cancer* **81**, 918-922.

Mullins, R. D., Heuser, J. A. and Pollard, T. D. (1998). The interaction of Arp2/3 complex with actin: nucleation, high affinity pointed end capping, and formation of branching networks of filaments. *Proc. Natl. Acad. Sci. USA* **95**, 6181-6186.

Pelham, R. J., Jr and Wang, Y. (1999). High resolution detection of mechanical forces exerted by locomoting fibroblasts on the substrate. *Mol. Biol. Cell* **10**, 935-945.

Petersen, N. O., McConnaughey, W. B. and Elson, E. L. (1982). Dependence of locally measured cellular deformability on position on the cell, temperature, and cytochalasin B. *Proc. Natl. Acad. Sci. USA* **79**, 5327-53231.

Pollard, T. D. and Cooper, J. A. (1986). Actin and actin-binding proteins. A critical evaluation of mechanisms and functions. *Annu. Rev. Biochem.* **55**, 987-1035.

Putman, C. A., van der Werf, K. O., de Grooth, B. G., van Hulst, N. F. and Greve, J. (1994). Viscoelasticity of living cells allows high resolution imaging by tapping mode atomic force microscopy. *Biophys. J.* **67**, 1749-53.

Rotsch, C. and Radmacher, M. (2000). Drug-induced changes of cytoskeletal structure and mechanics in fibroblasts: an atomic force microscopy study. *Biophys. J.* **78**, 520-535.

Sato, N., Funayama, N., Nagafuchi, A., Yonemura, S. and Tsukita, S. (1992). A gene family consisting of ezrin, radixin and moesin. Its specific localization at actin filament/plasma membrane association sites. *J. Cell Sci.* **103**, 131-143.

Schafer, D. A., Welch, M. D., Machesky, L. M., Bridgman, P. C., Meyer, S. M. and Cooper, J. A. (1998). Visualization and molecular analysis of actin assembly in living cells. *J. Cell Biol.* **143**, 1919-1930.

Shuster, C. B. and Herman, I. M. (1995). Indirect association of ezrin with F-actin: isoform specificity and calcium sensitivity. *J. Cell Biol.* **128**, 837-848.

Shuster, C. B., Lin, A. Y., Nayak, R. and Herman, I. M. (1996). Beta cap73: a novel beta actin-specific binding protein. *Cell Motil. Cytoskel.* **35**, 175-187.

Spector, I., Shochet, N. R., Blasberger, D. and Kashman, Y. (1989). Latrunculins–novel marine macrolides that disrupt microfilament organization and affect cell growth: I. Comparison with cytochalasin D. *Cell Motil. Cytoskel.* **13**, 127-144.

Theodoropoulos, P. A., Gravanis, A., Tsapara, A., Margioris, A. N., Papadogiorgaki, E., Galanopoulos, V. and Stournaras, C. (1994). Cytochalasin B may shorten actin filaments by a mechanism independent of barbed end capping. *Biochem. Pharmacol.* **47**, 1875-1881.

Thoumine, O. and Ott, A. (1997). Time scale dependent viscoelastic and contractile regimes in fibroblasts probed by microplate manipulation. *J. Cell Sci.* **110**, 2109-2116.

Tsuda, Y., Yasutake, H., Ishijima, A. and Yanagida, T. (1996). Torsional rigidity of single actin filaments and actin-actin bond breaking force under torsion measured directly by in vitro micromanipulation. *Proc. Natl. Acad. Sci. USA* **93**, 12937-12942.

Vaheri, A., Carpen, O., Heiska, L., Helander, T. S., Jaaskelainen, J., Majander-Nordenswan, P., Sainio, M., Timonen, T. and Turunen, O. (1997). The ezrin protein family: membrane-cytoskeleton interactions and disease associations. *Curr. Opin. Cell Biol.* **9**, 659-666.

Verkhovsky, A. B., Svitkina, T. M. and Borisy, G. G. (1997). Polarity sorting of actin filaments in cytochalasin-treated fibroblasts. *J. Cell Sci.* **110**, 1693-1704.

Wakatsuki, T., Kolodney, M. S., Zahalak, G. I. and Elson, E. L. (2000). Cell mechanics studied by a reconstituted model tissue. *Biophys. J.* **79**, 2353-2368.

Wang, N., Butler, J. P. and Ingber, D. E. (1993). Mechanotransduction across the cell surface and through the cytoskeleton. *Science* **260**, 1124-1127.

Zahalak, G. I., McConnaughey, W. B. and Elson, E. L. (1990). Determination of cellular mechanical properties by cell poking, with an application to leukocytes. *J. Biomech. Eng.* **112**, 283-294.

Zahalak, G. I., Wagenseil, Wakatsuki, T. and Elson, E. L. (2000). A cell-based constitutive relation for bio-artificial tissues. *Biophys. J.* **79**, 2369-2381.

Ziemann, F., Radler, J. and Sackmann, E. (1994). Local measurements of viscoelastic moduli of entangled actin networks using an oscillating magnetic bead micro-rheometer. *Biophys. J.* **66**, 2210-2216.